

See discussions, stats, and author profiles for this publication at: <https://www.researchgate.net/publication/221733655>

# Alkyne-Functionalized Ruthenium Nanoparticles: Ruthenium-Vinylidene Bonds at the Metal-Ligand Interface

ARTICLE in JOURNAL OF THE AMERICAN CHEMICAL SOCIETY · JANUARY 2012

Impact Factor: 12.11 · DOI: 10.1021/ja209568v · Source: PubMed

CITATIONS

24

READS

32

## 4 AUTHORS, INCLUDING:



**Xiongwu Kang**

Georgia Institute of Technology

28 PUBLICATIONS 344 CITATIONS

SEE PROFILE



**Joseph P Konopelski**

University of California, Santa Cruz

90 PUBLICATIONS 1,697 CITATIONS

SEE PROFILE



**Shaowei Chen**

University of California, Santa Cruz

218 PUBLICATIONS 7,482 CITATIONS

SEE PROFILE

## Alkyne-Functionalized Ruthenium Nanoparticles: Ruthenium–Vinylidene Bonds at the Metal–Ligand Interface

Xiongwu Kang, Nathaniel B. Zuckerman, Joseph P. Konopelski, and Shaowei Chen\*

Department of Chemistry and Biochemistry, University of California, 1156 High Street, Santa Cruz, California 95064, United States

## S Supporting Information

**ABSTRACT:** Stable ruthenium nanoparticles were prepared by the self-assembly of 1-dodecyne onto the “bare” Ru colloid surface. The formation of a Ru–vinylidene ( $\text{Ru}=\text{C}=\text{CH}-\text{R}$ ) interfacial bonding linkage was confirmed by the specific reactivity of the nanoparticles with imine derivatives to form a heterocyclic complex at the metal–ligand interface, as manifested in  $^1\text{H}$  and  $^{13}\text{C}$  NMR, photoluminescence, and electrochemical measurements in which a ferrocenyl imine was used as the labeling probe. Notably, the resulting nanoparticles could also undergo olefin metathesis reactions with vinyl-terminated molecules, as exemplified by the functionalization of the nanoparticles with 1-vinylpyrene. In sharp contrast, no reactivity was observed with 1-dodecynide-stabilized ruthenium nanoparticles with either imine or vinyl derivatives, indicating that these (deprotonated) nanoparticles were stabilized instead by the formation of a  $\text{Ru}-\text{C}\equiv\text{d}\pi$  bond at the metal–ligand interface.

Recently, metal–ligand interfacial bonding interactions have been recognized as a valuable and powerful parameter that plays an important role in the regulation of the nanoparticle material properties. This is rendered possible by the exploitation of metal–carbon covalent linkages for nanoparticle surface functionalization. Significantly, with conjugated interfacial bonds, extensive intraparticle charge delocalization may occur between particle-bound functional moieties, leading to the emergence of unprecedented optical and electronic properties. For instance, when ferrocenyl moieties are bound onto ruthenium nanoparticle surfaces by  $\text{Ru}=\text{carbene } \pi$  bonds, apparent intervalence charge transfer between the ferrocenyl metal centers at mixed valence is observed, as clearly manifested in electrochemical and near-IR spectroscopic measurements.<sup>1,2</sup> The behaviors are analogous to those observed in organometallic complexes with multiple metal centers bridged by conjugated linkers.<sup>3–8</sup> Intraparticle charge delocalization has also been observed with fluorophores such as pyrene and anthracene that are attached to the nanoparticle surface by similar  $\text{Ru}=\text{carbene } \pi$  bonds, whereby the particle-bound fluorophores exhibit emission characteristics that are consistent with those of their dimeric derivatives.<sup>9–11</sup> More recently, we demonstrated that effective intraparticle charge delocalization might also be achieved with nanoparticles functionalized by acetylide derivatives through the formation of metal–acetylide ( $\text{M}-\text{C}\equiv$ )  $\text{d}\pi$  linkages.<sup>12</sup>

In these earlier studies, the metal cores were found to serve as the conducting media that facilitate extended conjugation between the particle-bound functional moieties.<sup>1</sup> Therefore, intraparticle charge delocalization can be further manipulated by the deliberate variation of the energy structures of nanoparticle core electrons that may be afforded by simple chemical redox titration, electrostatic polarization, or photo-irradiation.<sup>13–15</sup>

Recently, we found that stable ruthenium nanoparticles could also be formed by the self-assembly of 1-alkyne molecules onto “bare” Ru colloids. This is different from those<sup>12</sup> stabilized by acetylide derivatives (i.e., deprotonated alkynes) by virtue of the  $\text{Ru}-\text{C}\equiv\text{d}\pi$  bonds,<sup>12</sup> which takes advantage of the isoelectronic character of the acetylide moieties with isocyanide. In contrast, the bonding nature of self-assembled 1-alkynes onto Ru nanoparticle surfaces has remained not well understood. This is the primary motivation of the present study.

It should be noted that self-assembly of alkynes on metal surfaces has been reported previously, although most of these early studies are confined to group IB metals of gold, silver, and copper that exhibit a  $\text{d}^{10}$  electronic structure. However, the chemical nature of the molecular adsorption remains under debate. For instance, Weaver and co-workers<sup>16,17</sup> employed surface-enhanced Raman spectroscopy (SERS) to investigate the adsorption of alkynes onto Au and Ag surfaces; on the basis of the frequency shifts of the  $-\text{C}\equiv\text{C}-$  and  $\equiv\text{C}-\text{H}$  vibrations, they argued that the alkynes were chemisorbed to the metals by  $\sigma\pi$  bonding. In this structural model, the overlap of a filled  $\pi$  orbital of the alkyne with an empty  $s$  orbital of the metal produces the  $\sigma$  component, whereas the  $\pi$  component is generated by the overlap of an empty  $\pi^*$  orbital of the alkyne with a filled metal  $d$  orbital. Such  $\sigma\pi$  bonding dictates that the  $-\text{C}\equiv\text{C}-$  triple bonds adopt a flat configuration on the metal surface so that the  $\pi$  orbitals are directed toward the metal surface plane.

In a more recent study, however, Zhang et al.<sup>18</sup> prepared self-assembled monolayers of terminal alkynes on gold, and on the basis of electrochemical and IR spectroscopic measurements, they proposed an upright orientation of the alkynes on the gold surface via an “undetermined” end-on interaction between the alkynes and gold. Such a configuration was also identified as the most stable mode of adsorption by Ford and co-workers,<sup>19</sup> who employed density functional theory to examine the adsorption energetics of ethynylbenzene on Au(111) and proposed the

Received: October 11, 2011

Published: January 3, 2012

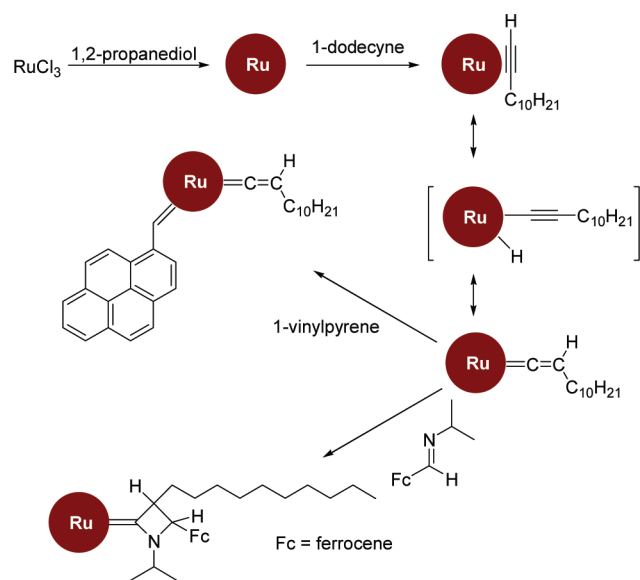
formation of a vinylidene surface-bound species by a 1,2-hydrogen shift.

In organometallic chemistry, the reactions of alkynes with transition-metal centers have been rather extensively studied; the potential products include  $\pi$ -alkyne, hydridoalkynyl, and vinylidene complexes, depending on the metals and the ligand environment.<sup>20,21</sup> The reaction mechanism typically involves an initial step where the alkyne molecule binds to the metal center in an  $\eta^2$  configuration. The complex can then undergo tautomeric rearrangements to produce hydride alkynyl (C–H oxidative addition) and/or vinylidene (1,3-hydrogen shift/1,2-hydrogen shift) derivatives. From the energetic point of view, it is generally accepted that the  $\pi$ -alkyne and vinylidene forms represent the kinetic and thermodynamic products, respectively, with the hydridoalkynyl form as an intermediate species.<sup>22,23</sup>

Therefore, an immediate question arises: in transition-metal nanoparticles stabilized by the self-assembly of 1-alkynes, will such a dynamic equilibrium also exist at the metal–ligand interface? This was addressed in the present study by taking advantage of the specific reactivity of metal–vinylidene complexes with imine derivatives to produce heterocyclic azetidinyldene complexes (in fact, this is the method of choice for identifying metal–vinylidene linkages in organometallic complexes).<sup>24</sup> Ruthenium nanoparticles stabilized by acetylide derivatives<sup>12</sup> were used as a comparative example. Because of the lack of  $\equiv\text{C–H}$  protons, no Ru–vinylidene bond would be anticipated to form at the nanoparticle interface, and thus, no reactivity with imine derivatives should be observed.

Experimentally, as depicted in Scheme 1, 1-dodecynyl-stabilized ruthenium (RuHC12, **1**) nanoparticles were used as

Scheme 1



the illustrating example. They were synthesized by the self-assembly of 1-dodecynyl onto the surface of “bare” Ru colloids that were prepared by thermolytic reduction of ruthenium(III) chloride (RuCl<sub>3</sub>) in 1,2-propanediol according to the procedure reported previously.<sup>1,9,10,25</sup> Transmission electron microscopy (TEM) measurements showed that the resulting nanoparticles exhibited an average core diameter of  $2.12 \pm 0.72$  nm.<sup>25</sup> The synthesis of 1-dodecynyl-stabilized ruthenium (RuHC12, **2**)

nanoparticles (diameter  $2.55 \pm 0.15$  nm) has been described previously.<sup>12</sup> Details of the synthesis of these nanoparticles are included in the Supporting Information (SI).

As mentioned above, if the terminal alkynes are initially anchored onto the Ru particle surface by the  $\eta^2$  configuration (which is generally stable at low temperatures), it is most likely that the surface bonding mode will be converted spontaneously to the vinylidene form (Ru=C=CH–R) at ambient temperature.<sup>22,23</sup> Since the vinylidene moiety reacts specifically with imine derivatives to form a heterocyclic azetidinyldene complex,<sup>24</sup> one may exploit this unique chemistry for nanoparticle surface labeling and functionalization. In the present study, we used a ferrocenyl imine as the labeling reagent, as depicted in Scheme 1.

Figure 1 shows the <sup>1</sup>H NMR spectra of the RuHC12 nanoparticles **1** (A) before and (B) after reactions with [(1-

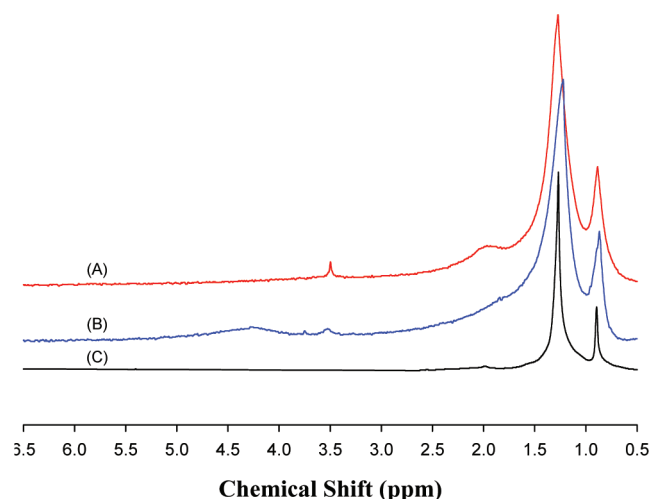


**Figure 1.** <sup>1</sup>H NMR spectra of the RuHC12 nanoparticles **1** (A) before and (B) after reactions with Fc-imine and (C) the RuC12 nanoparticles **2** after reactions with Fc-imine. The nanoparticles were all dissolved in CDCl<sub>3</sub>.

methylethylimino]methyl]ferrocene (Fc-imine, which was synthesized using a literature protocol<sup>26</sup> as detailed in the SI). It can be seen that both spectra exhibit a prominent broad peak at 0.9 ppm, which can be assigned to the terminal methyl (CH<sub>3</sub>) protons of the dodecynyl molecules, whereas (part of) the methylene (CH<sub>2</sub>) protons can be identified by the peak centered at 1.2 ppm [the peak at ca. 2 ppm in curve (A) diminished drastically after the nanoparticles reacted with Fc-imine, as depicted in curve (B); the origin of this peak is not clear at this point]. Importantly, the absence of sharp features in the NMR spectra indicates that the nanoparticle samples were spectroscopically clean and free of any excess ligands (similar behaviors were observed in <sup>13</sup>C NMR measurements; see Figure S1 in the SI).<sup>1,9,10,25</sup> Such a signatory behavior has been observed previously in organically capped nanoparticles and used extensively for the evaluation of nanoparticle purity.<sup>27</sup>

A closer examination of these two spectra shows that whereas no other meaningful features can be found with the RuHC12 nanoparticles **1** in curve (A) (the peak at 3.5 ppm is likely due to a trace amount of methanol), there is a broad peak at 3.9–4.5 ppm in curve (B) after the nanoparticles reacted with Fc-imine. This may be assigned to the ferrocenyl protons (Figure S2). Again, the appearance of only a broad peak (i.e., no sharp

features) in this region suggests that the ferrocenyl moiety was indeed successfully incorporated onto the nanoparticle surface (Scheme 1), with no contributions from excess ferrocenyl monomers. This strongly suggests that indeed the alkyne molecules self-assembled onto the Ru nanoparticle surface to form a Ru–vinylidene ( $\text{Ru}=\text{C}=\text{CH}-\text{C}_{10}\text{H}_{21}$ ) interfacial bonding linkage (Scheme 1). Because of the close proximity to the nanoparticle cores, the ferrocenyl signals were extensively broadened,<sup>27</sup> rendering it difficult to obtain an accurate quantification of the loading of ferrocenyl moieties on the nanoparticle surface, although it is anticipated to be low because of tight packing of the alkyne molecules on the nanoparticle surface.

In sharp contrast, for the (deprotonated) RuC12 nanoparticles **2**, only a featureless profile can be seen in the region between 3.9 and 4.5 ppm (again, the broad peaks centered at 0.9 and 1.2 ppm are ascribed to the methyl and part of the methylene protons, respectively), as depicted in curve (C), clearly indicating the lack of reactivity of the nanoparticles toward imine derivatives because of the absence of a vinylidene moiety at the metal–ligand interface.

The successful incorporation of the ferrocenyl moieties onto surface of the RuHC12 nanoparticles **1** was further confirmed by electrochemical measurements. Figure 2 shows differential

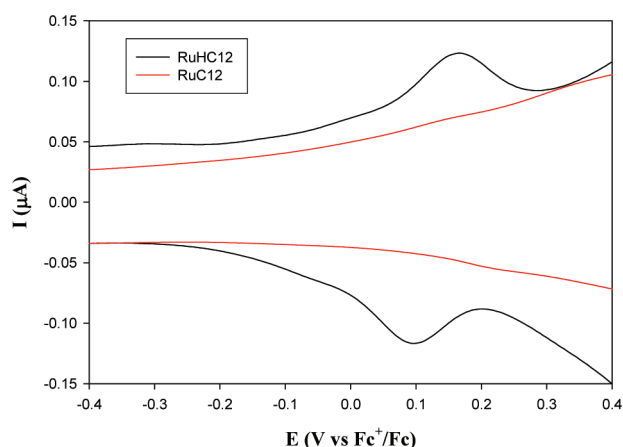


**Figure 2.** DPVs of RuHC12 nanoparticles **1** and RuC12 nanoparticles **2** after reactions with Fc-imine in  $\text{CH}_2\text{Cl}_2$  with 0.1 M TBAP. Conditions: nanoparticle concentration, 3 mg/mL; gold electrode surface area, 0.51  $\text{mm}^2$ ; DC ramp, 4 mV/s; pulse amplitude, 50 mV; pulse width, 200 ms. The potential was calibrated against the formal potential of ferrocene monomers in the same electrolyte solution.

pulse voltammograms (DPVs) of RuHC12 nanoparticles **1** (black curve) and RuC12 nanoparticles **2** (red curve) after reactions with Fc-imine. One can see that a pair of well-defined voltammetric peaks appears for **1** at a formal potential of ca. +0.13 V vs  $\text{Fc}^+/\text{Fc}$ . This is ascribed to the redox reactions ( $\text{Fc}^+ + \text{e}^- \rightleftharpoons \text{Fc}$ ) of ferrocenyl moieties incorporated into the nanoparticle surface-protecting layer (Scheme 1). The relatively large peak splitting ( $\Delta E_p \approx 70$  mV) and the apparent anodic shift of the formal potential relative to that of ferrocene monomers may be a result of the fact that the ferrocenyl moieties are surrounded by the hydrophobic ligand shell, as the energetically unfavorable environment would make it difficult for the counterions to reach the resulting ferrocenium ions and hence impede the electron-transfer kinetics.<sup>28</sup> In contrast, only a featureless profile was observed within the same potential

range for **2** after reaction with Fc-imine, which is again indicative of the lack of reactivity of the nanoparticles with imine derivatives.

The nanoparticle photoluminescence (PL) characteristics also exhibited marked differences with and without Fc-imine labeling. It has been reported that acetylide-functionalized Ru shows apparent fluorescence with excitation and emission maxima at 360 and 440 nm, respectively.<sup>12</sup> This arises from intraparticle charge delocalization between the particle-bound  $\text{C}\equiv\text{C}$  moieties as a result of the conjugated Ru– $\text{C}\equiv\text{C}$  interfacial bonding linkage. Consequently, the nanoparticle-bound  $\text{C}\equiv\text{C}$  groups behave analogously to diacetylene derivatives.<sup>12</sup> Similar PL characteristics were observed with the as-produced RuHC12 nanoparticles **1** (black curves in Figure 3), suggesting

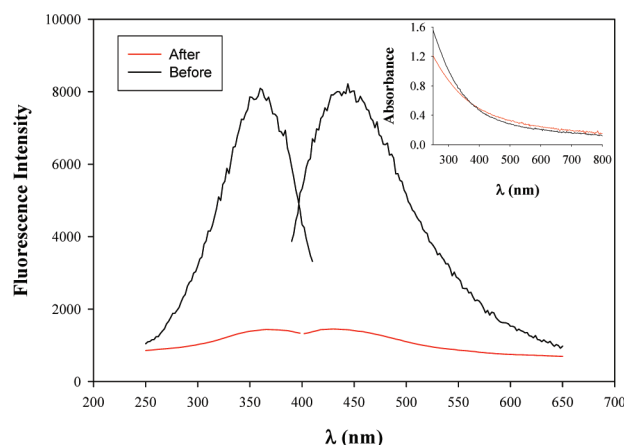


**Figure 3.** Excitation and emission spectra of RuHC12 nanoparticles **1** in  $\text{CH}_2\text{Cl}_2$  before (black curves) and after (red curves) reactions with Fc-imine. The corresponding UV–vis absorption spectra are shown in the inset. The nanoparticle concentration was 0.1 mg/mL.

conjugated character in the metal–ligand interfacial bonding interactions. More significantly, upon labeling with Fc-imine, the PL diminished significantly by more than 5-fold (red curves), although the optical density of **1** remained virtually unchanged before and after reactions with Fc-imine (Figure 3 inset). This is again consistent with the formation of a heterocyclic complex on the nanoparticle surface that converts the Ru–vinylidene linkage to a simple  $\text{Ru}=\text{C}$  carbene one (Scheme 1), which is inactive in fluorescence.

The experimental results presented above highlight the marked discrepancy of metal–ligand interfacial bonding interactions for RuHC12 nanoparticles **1** and RuC12 nanoparticles **2**. Specifically, the acetylide-functionalized nanoparticles **2** were most likely stabilized by the  $d\pi$  ( $\text{Ru}-\text{C}\equiv\text{C}$ ) interfacial bonding interactions between the metal cores and the  $\text{C}\equiv\text{C}$  moieties,<sup>12,13</sup> whereas active tautomerization involving an equilibrium between the metal– $\eta^2$ -alkyne, hydridoalkynyl, and metal–vinylidene interfacial linkages occurred at the metal–ligand interface for the alkyne-stabilized nanoparticles **1** (Scheme 1).<sup>29</sup> Reactions with imine derivatives (e.g., ferrocenyl imine) led to an apparent shift of the equilibrium toward the metal–vinylidene form, which was also favored at ambient temperature.<sup>24</sup>

The difference between the metal–ligand interfacial bonding interactions for the RuHC12 nanoparticles **1** and RuC12 nanoparticles **2** is further manifested by the reactivity of the nanoparticles with vinyl-terminated derivatives in olefin meta-



thesis reactions.<sup>30</sup> Experimentally, we observed that with a Ru–acetylide (Ru–C≡) interfacial bond, nanoparticles **2** might undergo ligand exchange reactions with alkynide anions; however, the nanoparticles showed little reactivity with vinyl-terminated molecules.<sup>12</sup> In sharp contrast, nanoparticles **1** could be readily functionalized with molecules having a vinyl terminus. We used 1-vinylpyrene as the illustrating example in the present study. Figure 4 shows the excitation and emission

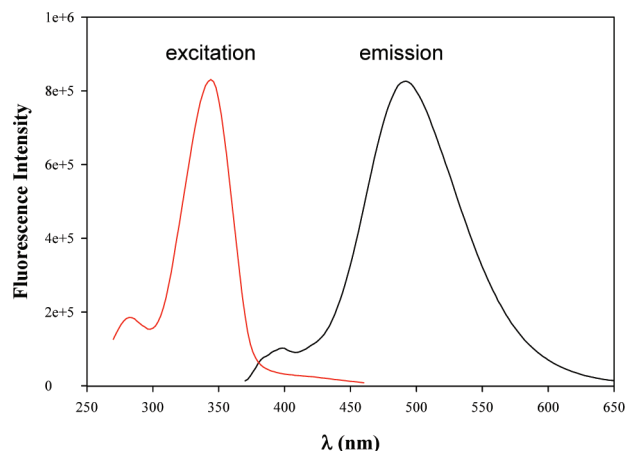


**Figure 4.** Excitation and emission spectra of RuHC12 nanoparticles **1** after the olefin metathesis reaction with 1-vinylpyrene in CH<sub>2</sub>Cl<sub>2</sub>. The nanoparticle concentration was 0.1 mg/mL.

spectra of nanoparticles **1** after reactions with 1-vinylpyrene. It can be seen that the fluorescence profiles are consistent with those observed with pyrene-functionalized Ru nanoparticles having Ru=carbene  $\pi$  bonds.<sup>9</sup> Significantly, the emission spectrum shows a prominent peak at 492 nm along with a small one at ca. 392 nm, which is ascribed to the extended conjugation between the particle-bound pyrene moieties arising from the conjugated metal–ligand interfacial bonding interactions, allowing the pyrene moieties to behave analogously to their dimeric counterparts with a conjugated spacer.<sup>9</sup> Again, the successful incorporation of vinylpyrene onto the nanoparticle surface further confirms the formation of a Ru–vinylidene interfacial linkage with nanoparticles **1**.

In summary, stable ruthenium nanoparticles were prepared by the self-assembly of alkynes onto the “bare” Ru colloid surface by virtue of the formation of Ru–vinylidene interfacial bonding interactions (as manifested by NMR, electrochemical, and PL measurements), in contrast to the (deprotonated) alkynide-functionalized counterparts, which exhibited Ru–C≡d $\pi$  bonds at the metal–ligand interface. Importantly, with this interfacial bond, it is envisaged that the rich chemistry<sup>31–34</sup> observed with metal–vinylidene organometallic complexes may be exploited for unprecedented functionalization and manipulation of the nanoparticle structures and properties. Research toward this end is underway.

## ■ ASSOCIATED CONTENT

### Supporting Information

Experimental details; procedures for the syntheses of **1**, **2**, and Fc-imine; and additional NMR spectra. This material is available free of charge via the Internet at <http://pubs.acs.org>.

## ■ AUTHOR INFORMATION

### Corresponding Author

shaowei@ucsc.edu

## ■ ACKNOWLEDGMENTS

This work was supported by NSF (CHE-0832605 and CHE-1012258) and ACS PRF (49137-ND10).

## ■ REFERENCES

- (1) Chen, W.; Chen, S. W.; Ding, F. Z.; Wang, H. B.; Brown, L. E.; Konopelski, J. P. *J. Am. Chem. Soc.* **2008**, *130*, 12156.
- (2) Chen, W.; Brown, L. E.; Konopelski, J. P.; Chen, S. W. *Chem. Phys. Lett.* **2009**, *471*, 283.
- (3) Cowan, D. O.; Levanda, C.; Park, J.; Kaufman, F. *Acc. Chem. Res.* **1973**, *6*, 1.
- (4) Day, P.; Hush, N. S.; Clark, R. J. H. *Philos. Trans. R. Soc., A* **2008**, *366*, 5.
- (5) Gamelin, D. R.; Bominaar, E. L.; Mathoniere, C.; Kirk, M. L.; Wieghardt, K.; Girerd, J. J.; Solomon, E. I. *Inorg. Chem.* **1996**, *35*, 4323.
- (6) Williams, R. D.; Petrov, V. I.; Lu, H. P.; Hupp, J. T. *J. Phys. Chem. A* **1997**, *101*, 8070.
- (7) Brunschwig, B. S.; Creutz, C.; Sutin, N. *Chem. Soc. Rev.* **2002**, *31*, 168.
- (8) Sun, H.; Steeb, J.; Kaifer, A. E. *J. Am. Chem. Soc.* **2006**, *128*, 2820.
- (9) Chen, W.; Zuckerman, N. B.; Lewis, J. W.; Konopelski, J. P.; Chen, S. W. *J. Phys. Chem. C* **2009**, *113*, 16988.
- (10) Chen, W.; Zuckerman, N. B.; Konopelski, J. P.; Chen, S. W. *Anal. Chem.* **2010**, *82*, 461.
- (11) Chen, W.; Pradhan, S.; Chen, S. W. *Nanoscale* **2011**, *3*, 2294.
- (12) Chen, W.; Zuckerman, N. B.; Kang, X. W.; Ghosh, D.; Konopelski, J. P.; Chen, S. W. *J. Phys. Chem. C* **2010**, *114*, 18146.
- (13) Kang, X. W.; Zuckerman, N. B.; Konopelski, J. P.; Chen, S. W. *Angew. Chem., Int. Ed.* **2010**, *49*, 9496.
- (14) Kang, X. W.; Chen, W.; Zuckerman, N. B.; Konopelski, J. P.; Chen, S. W. *Langmuir* **2011**, *27*, 12636.
- (15) Song, Y.; Kang, X. W.; Zuckerman, N. B.; Phebus, B.; Konopelski, J. P.; Chen, S. W. *Nanoscale* **2011**, *3*, 1984.
- (16) Patterson, M. L.; Weaver, M. J. *J. Phys. Chem.* **1985**, *89*, 5046.
- (17) Feilchenfeld, H.; Weaver, M. J. *J. Phys. Chem.* **1989**, *93*, 4276.
- (18) Zhang, S.; Chandra, K. L.; Gorman, C. B. *J. Am. Chem. Soc.* **2007**, *129*, 4876.
- (19) Ford, M. J.; Hoft, R. C.; McDonagh, A. J. *Phys. Chem. B* **2005**, *109*, 20387.
- (20) Bruce, M. I. *Chem. Rev.* **1998**, *98*, 2797.
- (21) Bruneau, C.; Dixneuf, P. H. *Acc. Chem. Res.* **1999**, *32*, 311.
- (22) Bianchini, C.; Peruzzini, M.; Vacca, A.; Zanolini, F. *Organometallics* **1991**, *10*, 3697.
- (23) Bullock, R. M. *J. Chem. Soc., Chem. Commun.* **1989**, 165.
- (24) Zayed, M. A.; Fischer, H. J. *Therm. Anal. Calorim.* **2000**, *61*, 897.
- (25) Chen, W.; Davies, J. R.; Ghosh, D.; Tong, M. C.; Konopelski, J. P.; Chen, S. W. *Chem. Mater.* **2006**, *18*, 5253.
- (26) Balogh, J.; Kegl, T.; Parkanyi, L.; Kollar, L.; Ungvary, F.; Skoda-Foldes, R. *J. Organomet. Chem.* **2011**, *696*, 1394.
- (27) Hostetler, M. J.; Wingate, J. E.; Zhong, C. J.; Harris, J. E.; Vachet, R. W.; Clark, M. R.; Londono, J. D.; Green, S. J.; Stokes, J. J.; Wignall, G. D.; Glish, G. L.; Porter, M. D.; Evans, N. D.; Murray, R. W. *Langmuir* **1998**, *14*, 17.
- (28) Rowe, G. K.; Creager, S. E. *J. Phys. Chem.* **1994**, *98*, 5500.
- (29) Bustelo, E.; de los Rios, I.; Tenorio, M. J.; Puerta, M. C.; Valerga, P. *Monatsh. Chem.* **2000**, *131*, 1311.
- (30) Tulevski, G. S.; Myers, M. B.; Hybertsen, M. S.; Steigerwald, M. L.; Nuckolls, C. *Science* **2005**, *309*, 591.
- (31) Bianchini, C.; Masi, D.; Romero, A.; Zanolini, F.; Peruzzini, M. *Organometallics* **1999**, *18*, 2376.
- (32) Wakatsuki, Y. *J. Organomet. Chem.* **2004**, *689*, 4092.
- (33) Dragutan, V.; Dragutan, I. *Platinum Met. Rev.* **2004**, *48*, 148.
- (34) Fruhauf, H. W. *Chem. Rev.* **1997**, *97*, 523.